EFFECTIVE AREA OF SXT MIRROR (IN-FLIGHT)

J. R. Lemen
17 Dec 1992, Rev B

This note describes the effective area of the SXT mirror that is used for the determination of the SXT response function. This note is an update on L. W. Acton's Calibration Note 25.

In SXT Calibration Note 14 we described a very simple meridional ray trace model for the SXT mirror, based on the originally specified hyperboloid-hyperboloid parameters, and modified semi-empirically to agree with the measured cone angles and with the focus results from the June 1989 tests at MSFC (MSFC2).

This model was used to predict the mirror reflectivity. These results were linearly interpolated to the actual measurements. The details are explained below. The curve labelled "a" in Figure 3 and given numerically in Table 5 should be used as the SXT effective area as a function of wavelength.

A. MEASUREMENTS

During the MSFC2 calibration in June 1989, the effective area of the SXT telescope was measured at 11 wavelengths. The results of the analysis are given in Table 1. Table 2 contains the raw data that was recorded on Pages 71-72 of the MSFC2 log book. The measurements at MSFC were performed by R. C. Catura, B. K. Jurcevich, M. D. Morrison, and J. R. Lemen.

Table 1: SXT Measured Mirror area (cm^2) from MSFC 2 (June 1989)

E(keV)	(Ang)	cm^2	+/-	#	Line	Measured/Theory*
0.277	44.76	1.722	0.009	8	C K	0.998255
0.525	23.62	1.551	0.023	1	O K	0.987445
0.573	21.64	1.472	0.017	1	Cr L	0.946624
0.705	17.59	1.460	0.017	1	Fe L	0.954891
0.930	13.33	1.420	0.010	9	Cu L	0.932725
1.490	8.32	1.454	0.008	9	Al K	0.961933
1.740	7.13	1.320	0.014	1	Si K	0.914336
2.040	6.08	1.079	0.012	1	Zr L	0.890132
2.980	4.16	0.219	0.002	3	Ag L	0.552194
3.440	3.60	0.132	0.002	1	Sn L	0.421394
4.510	2.75	0.0158	0.0002	1	Ti K	0.229516

*Theory refers to Theory Calculation 1 (MSFC source distance and MSFC obscuration). See section B.

Table 2: MSFC Mirror Effective Area Data (June 1989)

E(keV)	(Ang)	OOC	(s)	OCC	(s)	OAO	(s)	OAC	(s)	Area+/-(cm^2)	Line
0.277	44.76	11412	40	15	200	2008	40	93	40	1.811 0.043	C K
0.277	44.76	11700	40	15	200	2069	40	50	40	1.761 0.042	C K
0.277	44.76	58111	200	15	200	10517	200	50	40	1.720 0.018	C K
0.277	44.76	10316	40	15	200	9478	200	50	40	1.699 0.024	C K
0.277	44.76	10293	40	12	200	9435	200	56	40	1.709 0.024	C K
0.277	44.76	10346	40	14	200	9492	200	51	40	1.702 0.024	C K
0.277	44.76	10107	40	14	200	9068	200	57	40	1.749 0.025	C K
0.277	44.76	10393	40	15	200	9516	200	60	40	1.714 0.024	C K
0.525	23.62	12277	200	31	200	7452	600	83	200	1.551 0.023	O K
0.573	21.64	19537	200	24	200	12447	600	60	100	1.472 0.017	Cr L
0.705	17.59	18350	400	18	200	11811	1200	62	200	1.460 0.017	Fe L
0.930	13.33	2269	20	40	40	935	40	42	40	1.531 0.058	Cu L
0.930	13.33	2330	20	40	40	1036	40	34	40	1.402 0.052	Cu L
0.930	13.33	2614	20	40	40	1145	40	37	40	1.423 0.050	Cu L
0.930	13.33	2563	20	40	40	1176	40	34	40	1.354 0.047	Cu L
0.930	13.33	2467	20	40	40	1089	40	33	40	1.409 0.051	Cu L
0.930	13.33	2369	20	40	40	5361	200	32	40	1.373 0.034	Cu L
0.930	13.33	2178	20	40	40	5127	200	31	40	1.319 0.034	Cu L
0.930	13.33	23642	200	40	40	10393	400	174	200	1.419 0.017	Cu L
0.930	13.33	11681	100	40	40	9864	400	81	100	1.476 0.020	Cu L
1.490	8.32	9800	20	41	40	2227	20	80	20	1.385 0.032	Al K
1.490	8.32	20663	40	41	40	4573	40	161	40	1.421 0.023	Al K
1.490	8.32	9549	20	41	40	2059	20	77	20	1.461 0.035	Al K
1.490	8.32	6790	20	41	40	2791	40	111	40	1.536 0.034	Al K
1.490	8.32	8369	20	41	40	3562	40	126	40	1.477 0.029	Al K
1.490	8.32	8232	20	41	40	3537	40	129	40	1.465 0.029	Al K
1.490	8.32	20704	40	32	200	4535	40	758	200	1.435 0.022	Al K
1.490	8.32	21378	40	25	200	11598	100	699	200	1.444 0.016	Al K
1.490	8.32	19955	40	32	200	10581	100	713	200	1.483 0.017	Al K
1.740	7.13	22078	200	31	200	15800	600	189	200	1.320 0.014	Si K
2.040	6.08	13809	40	37	200	20036	200	295	100	1.079 0.012	Zr L
2.980	4.16	10265	100	61	200	14304	100	272	200	0.220 0.003	Ag L
2.980	4.16	10127	100	65	200	14220	100	292	200	0.218 0.003	Ag L
2.980	4.16	10203	100	69	200	14180	100	264	200	0.220 0.003	Ag L
3.440	3.60	13579	400	56	200	15651	200	139	200	0.132 0.002	Sn L
4.510	2.75	25587	1200	79	200	16167	40	146	200	0.016 0.000	Ti K

Notes:
1. Area = .304 (cm^2) * (OOC-OCC) / (OAO-OAC)
2. .304 cm^2 corresponds to the hole diameter in the solid Al disk = .245 inch
3. d(Area) / Area = sqrt(1/OOC + 1/OAO)

The measurements were made using the proportional counter from the lab's high-energy monochromator, however, because of the measurement technique, the results are only weakly dependent on the proportional counter response.

The SXT at MSFC2 during these measurements did not have the aspect sensor installed. Furthermore, there was one position in the filter wheel which had a solid Al disk with a hole drilled in it having a known area (.304 cm^2). By inserting this disk with a hole, we were able to observe the X-ray beam through the aspect sensor opening and at the same time block the X-ray flux from the X-ray mirrors. Another filter position contained a solid Al disk which was used to obtained detector background count rates. Four different kinds of measurements were made (see Table 3):

Table 3: Key to measurements made at MSFC2

Key	Description	Filter Wheel	Aspect Sensor door
00C	= X-rays from mirror.	Open	Closed
0CC	= Detector background.	Closed	Closed
0A0	= Direct Beam (through .304 cm^-2 aperture)	.304 Hole	Open
0AC	= Background in 0A0 from X-rays scattered by mirror	.304 Hole	Closed

B. CALCULATED EFFECTIVE AREA

The ray tracing model (Ray2.pro) that was described in Calibration Note 14 was used to compute the reflectivity of the mirror. It used the adjusted mirror parameters (the values which gave the observed focal length) and an assumed coating of 450 Ang of Au deposited on 80 Ang of Cr. For the reflectivity calculation we used David Windt's LSMRT.pro program and the updated (received by W. A. Brown in Dec 1990) optical constants of Henke, Davis, Gullikson, and Perera. The reflectivities were computed as a function of energy. The reflectivity varies slightly depending upon the position that the ray strikes the front mirror along the longitudinal axis (the ray tracing model assumes axial symmetry) because of the corresponding variation in the incident angle of the ray. This variation is small, for example, only varying by 0.3% from one extreme to the other at 8.4 Ang. For the purpose of computing the theoretical effective area, the reflectivity at 31 positions along the longitudinal axis were computed and averaged for each wavelength.

The theoretical effective area was computed for the case of the MSFC source distance (Model 1) and for an source at infinity (Model 2). The reflectivities of these two cases are in very good agreement, with the main differences being at very short wavelengths where the reflectivity is small in any case.

The mirror is obscured slightly by the support structure and by the entrance filter holders. The instrument was not in its flight configuration during the MSFC2 testing so a slightly different obscuration must be used to obtain the effective area for the flight configuration.

Two theoretical models were computed:

Table 4: Description of Ray-Trace Calculations

	Source Distance	Area (in^2) (includes obscuration)	Obscuration
Theory Calculation 1:	MSFC Tube Length	.39713	.97883
Theory Calculation 2:	Infinity	.38090	.93882

The area was computed from the inner and outer radii of the useful mirror surface being given by (see Cal Note 14):

r1 = 4.526138 in
r2 = 4.540382 in

and the annulus area = .405720 in^2.

The obscuration factors were derived from CADAM printouts made by B. K. Jurcevich (also see Scott Claflin's message reproduced as an appendix).

C. RESULT: MIRROR EFFECTIVE AREA

Theory Calculation 1 was compared to the measured values. The ratios of the measured area to the theoretical calculation are shown in the last column of Table 1. Figure 1 shows the measured values as data points and the Theory Calculation 1 as a solid curve. Figure 2 shows the ratio of measured to Theory Calculation 1. The data points represent the values in the last column of Table 1. The dashed curve is the result of linear interpolation between the points. This curve was multiplied times Theory Calculation 2 (Infinity source distance and flight obscuration) and is shown as the "jagged" curve running through the data points and labelled "a" in Figure 3. In this case, the observed data has been multiplied by the ratio of the the obscurations (=.93882 / .97883). The solid curve above it is the Theory Calculation 2.

The Dashed curve above that is the mirror effective area that was used to compute the SXT response function in July 1991. This curve makes use of the infinity focus ray trace model, but uses the MSFC obscuration factor. This calculation is not appropriate and should not be used in future analyses.

Curve "a" was used in the SXT effective area calculation that was made in Dec 1992.

D. DISCUSSION

As one can see from Figures 1 and 2, there is a considerable disagreement between the MSFC2 measurements and Theory Calculation 1 for the short wavelengths. The cause for this, especially at short wavelengths, is most likely scattering, which has not been included in the theoretical calculation. At longer wavelengths, for example, above 6 Ang, the disagreement is of the order of 10% or less.

The measurements obtained during the MSFC2 tests were conducted so as to minimize the statistical error as much as possible. As a result, the uncertainties given in Table 1 are on average only 1% and the maximum uncertainty is only 1.5% (see Figure 4).

What are the causes then for the disagreement between the measurements and the theory? Although the statistical errors of the measurements are quite small, there may be unknown systematic errors. However, the simplicity of the measurement technique partially guards against systematic effects. Another cause might be errors in the optical constants that were used for gold and chromium or in the assumed layer thicknesses. Finally, we have not attempted to include scattering which will reduce the reflectivity, especially at shorter wavelengths.

One possible systematic effect is a drift in the MSFC X-ray beam flux with time. In the MSFC2 log book the beam intensity is recorded from the MSFC monitor proportional counter at various times throughout the testing. The X-ray source had good compensation and the typical flux variation for strong lines was approximately one percent per hour. The longest integration was 20 min for Fe L at 17.59 Ang. The beam intensity was changing by about 3.5% per hour during this measurement, and thus, the Fe L value may contain a 1% systematic effect from X-ray beam flux variation. A few energies required ten minute integrations. The Cr L line for example showed a 4% flux drift in a 20 min time interval as measured with the MSFC monitor counter during which the 10 min Cr L measurement was made. Assuming that this variation was nearly linear in time, then the Cr L measurement may contain a 2% systematic effect. The largest recorded variation is 5% for the Si K and O K lines. In summary, we conclude that the beam variation is not a significant systematic effect in these measurements.

Because the statistical uncertainties are so small, the approach we have adopted is to linearly interpolate the theoretical calculation to the MSFC2 measurements. Other "fitting" schemes (such as spline or polynomial interpolation) are possible, but since we have no detailed knowledge for the causes of the discrepancies, there is no justification for more sophistication than the linear treatment.

There is the question of what uncertainty we should assign to the mirror effective area for the purpose of calculating the uncertainty of the SXT response function. This is somewhat difficult, because of the unknown systematic problems discussed above. However, it is conservative to assume that the uncertainties are bounded by the statitical error (1%) at the lower limit and at the upper limit by the wavelength-dependent measured/theory (Table 1) fractions.

Finally, we stress that the curve labelled "a" in Figure 3 and given numerically in Table 5 should be used as the SXT effective area as a function of wavelength.

APPENDIX: E. Scott Claflin Memo

From: LPARL2::CLAFLIN 1-MAR-1991 01:46:38.71
To: SAG::LEMEN
CC:
Subj: SXT Obscuration Factor

>From: SAG::LEMEN 28-FEB-1991 14:02:19.06
>To: LOCKHD::CLAFLIN
>CC:
>Subj: SXT obscuration factor

>Hello Scott,

>Loren wanted me to produce a table of our "best guess" for the SXT mirror
>effective area. I am using the following number:

> .39713*2.54^2 cm^2

>I recall that this includes the obscuration for the MSFC test configuration.
>Is that correct? If so, what is the obscuration factor?

>Do you know what the appropriate value should be for the orbital configuration?
>(I think you and Bruce calculated that number on Cadam, but I can't find
>a record of it).

>Thanks,
>Jim

Jim,

I have the CADAM printout made by Bruce Jurcevich. The inner and outer radii of the useful mirror surface are given as

r1 = 4.526138 in
r2 = 4.540382 in

The annulus area is then

area = .405720 in^2

The areas diminished by obscuration were calculated by Cadam to be

MSFC_area = .39713 in^2
Flight_area = .38090 in^2

Dividing by the annulus area to get the obscuration factor

MSFC_obsc = .97883
Flight_obsc = .93882

Let me know if you need to look at the Cadam printout. --Scott C.

Table 5: SXT MIRROR EFFECTIVE AREA (Curve "a" in Fig. 3)

wave	cm^2	wave	cm^2
1.2399	1.4498e-06	3.8315	0.1719
1.2687	1.2905e-06	3.9207	0.1642
1.2983	6.3207e-06	4.0121	0.1888
1.3285	7.5089e-06	4.1055	0.2012
1.3595	1.5673e-05	4.2012	0.2118
1.3911	3.7111e-05	4.2991	0.2205
1.4235	1.1135e-05	4.3991	0.2099
1.4567	1.7538e-06	4.5017	0.2002
1.4906	1.2208e-05	4.6065	0.2597
1.5253	2.2711e-05	4.7137	0.2670
1.5609	8.6327e-06	4.8236	0.2742
1.5972	2.8812e-05	4.9359	0.2628
1.6344	5.2338e-05	5.0509	0.2529
1.6725	3.9089e-05	5.1686	0.2443
1.7115	4.9741e-05	5.2890	0.1942
1.7513	7.3670e-05	5.4121	0.1274
1.7921	8.1523e-05	5.5383	0.1549
1.8339	1.3205e-04	5.6671	1.0174e-03
1.8766	1.2616e-04	5.7991	0.7750
1.9203	1.2923e-04	5.9343	0.9296
1.9650	3.6066e-04	6.0726	1.033
2.0108	3.3774e-04	6.2139	1.099
2.0576	2.9519e-04	6.3589	1.129
2.1056	5.6701e-04	6.5067	1.176
2.1546	6.1847e-04	6.6583	1.195
2.2048	1.0904e-03	6.8135	1.230
2.2562	1.0393e-03	6.9721	1.241
2.3087	1.9643e-03	7.1346	1.266
2.3625	2.0206e-03	7.3010	1.291
2.4175	3.4548e-03	7.4708	1.314
2.4738	3.4082e-03	7.6449	1.333
2.5314	5.9283e-03	7.8229	1.350
2.5904	5.8959e-03	8.0052	1.364
2.6507	9.8420e-03	8.1914	1.376
2.7125	9.5988e-03	8.3825	1.394
2.7757	1.5189e-02	8.5779	1.400
2.8403	2.4920e-02	8.7777	1.404
2.9065	2.4987e-02	8.9818	1.406
2.9742	3.6984e-02	9.1909	1.405
3.0435	5.1380e-02	9.4049	1.402
3.1143	6.7668e-02	9.6247	1.406
3.1869	6.5325e-02	9.8487	1.407
3.2611	8.1307e-02	10.0780	1.407
3.3371	9.7585e-02	10.3120	1.405
3.4148	0.1137	10.5530	1.402
3.4944	0.1086	10.7980	1.402
3.5757	0.1234	11.0500	1.395
3.6591	0.1443	11.3070	1.392
3.7443	0.1584	11.5710	1.388

wave	cm^2	wave	cm^2
11.8410	1.383	34.9440	1.577
12.1160	1.379	35.7570	1.583
12.3990	1.375	36.5910	1.590
12.6870	1.374	37.4430	1.597
12.9830	1.368	38.3150	1.602
13.2850	1.362	39.2070	1.608
13.5950	1.365	40.1210	1.614
13.9110	1.368	41.0550	1.620
14.2350	1.374	42.0120	1.628
14.5670	1.376	42.9910	1.635
14.9060	1.380	43.9910	1.642
15.2530	1.381	45.0170	1.652
15.6090	1.384	46.0650	1.662
15.9720	1.387	47.1370	1.673
16.3440	1.390	48.2360	1.684
16.7250	1.391	49.3590	1.695
17.1150	1.396	50.5090	1.705
17.5130	1.400	51.6860	1.716
17.9210	1.402	52.8900	1.729
18.3390	1.401	54.1210	1.743
18.7660	1.400	55.3830	1.757
19.2030	1.400	56.6710	1.773
19.6500	1.401	57.9910	1.791
20.1080	1.403	59.3430	1.808
20.5760	1.407	60.7260	1.828
21.0560	1.410	62.1390	1.849
21.5460	1.412	63.5890	1.868
22.0480	1.428	65.0670	1.892
22.5620	1.447	66.5830	1.921
23.0870	1.467	68.1350	1.952
23.6250	1.488	69.7210	1.987
24.1750	1.489	71.3460	2.026
24.7380	1.492	73.0100	2.065
25.3140	1.496	74.7080	2.105
25.9040	1.502	76.4490	2.140
26.5070	1.505	78.2290	2.169
27.1250	1.510	80.0520	2.195
27.7570	1.517	81.9140	2.214
28.4030	1.522	83.8250	2.232
29.0650	1.529	85.7790	2.243
29.7420	1.535	87.7770	2.251
30.4350	1.541	89.8180	2.258
31.1430	1.547	91.9090	2.263
31.8690	1.552	94.0490	2.269
32.6110	1.558	96.2470	2.274
33.3710	1.563	98.4870	2.278
34.1480	1.570		

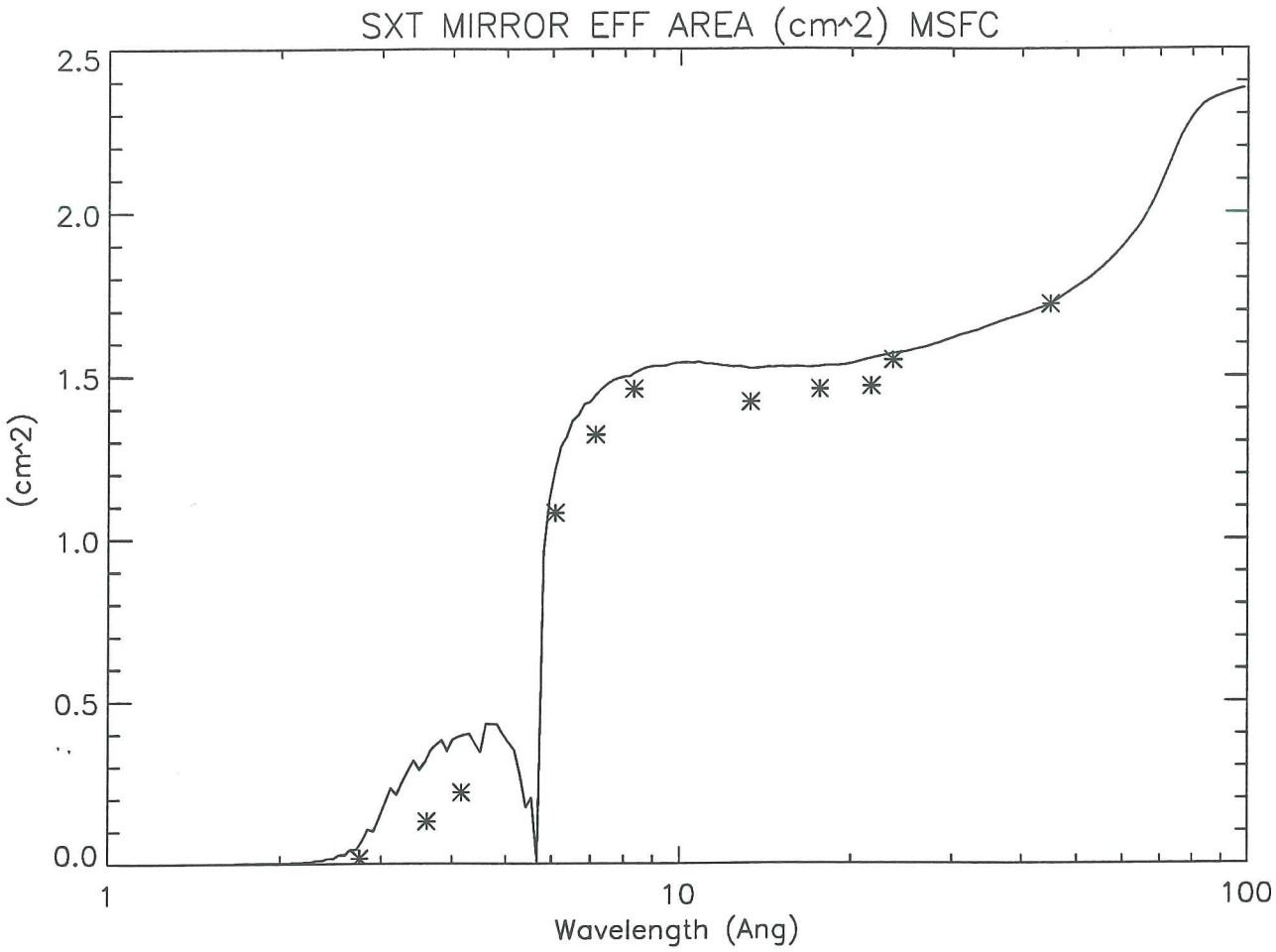

Figure 1: SXT mirror effective area at 11 wavelengths obtained during the June 1989 MSFC2 measurements. The solid curve is Theory Calculation 1 which assumes the MSFC source distance and the MSFC obscuration.

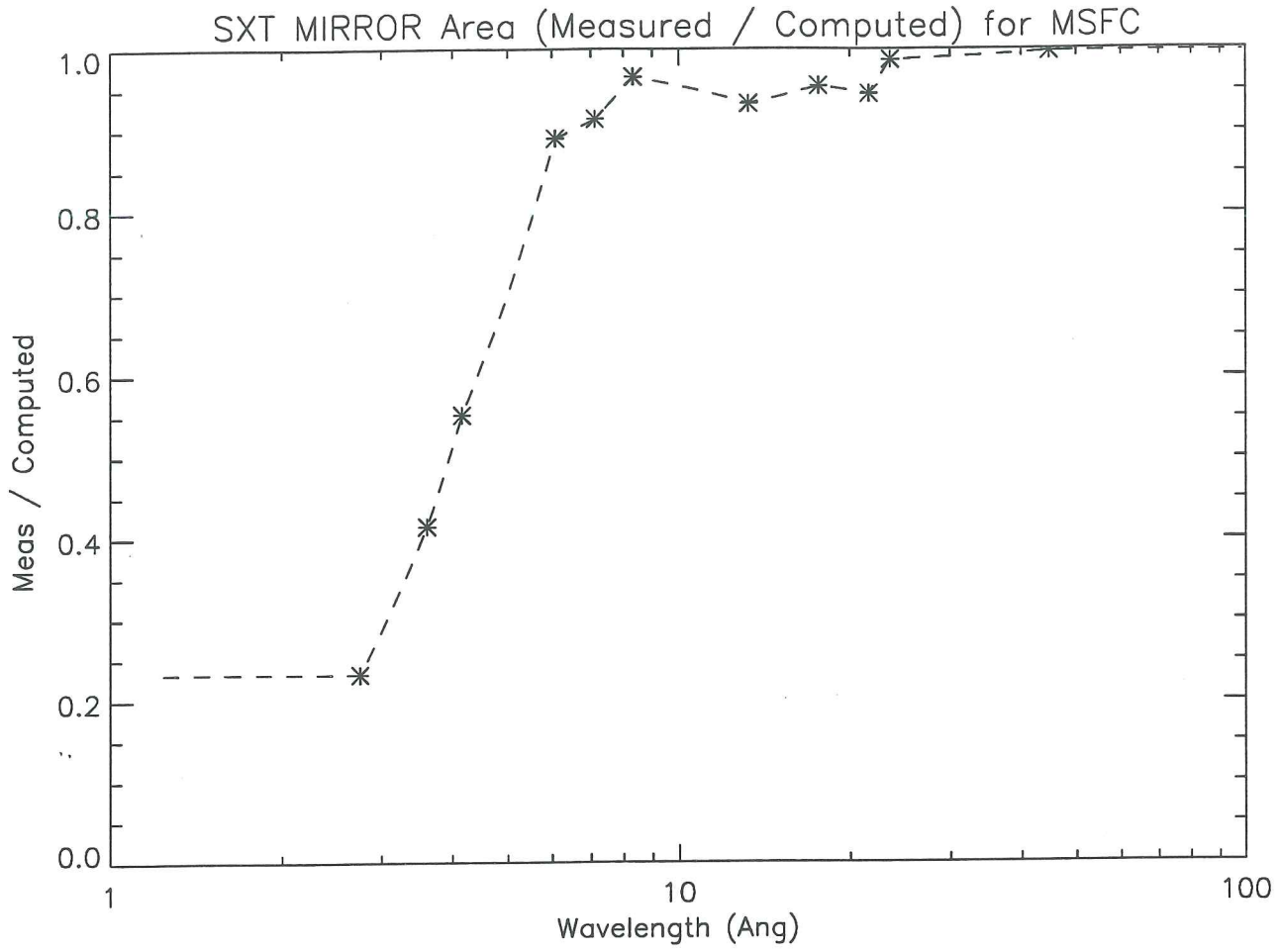

Figure 2: The ratio of the measured SXT mirror area at MSFC2 to Theory Calculation 1 which assumes the MSFC source distance and the MSFC obscuration. The dashed curve is a linear interpolation. This linear interpolation is the correction that is applied to Theory Calculation 2.

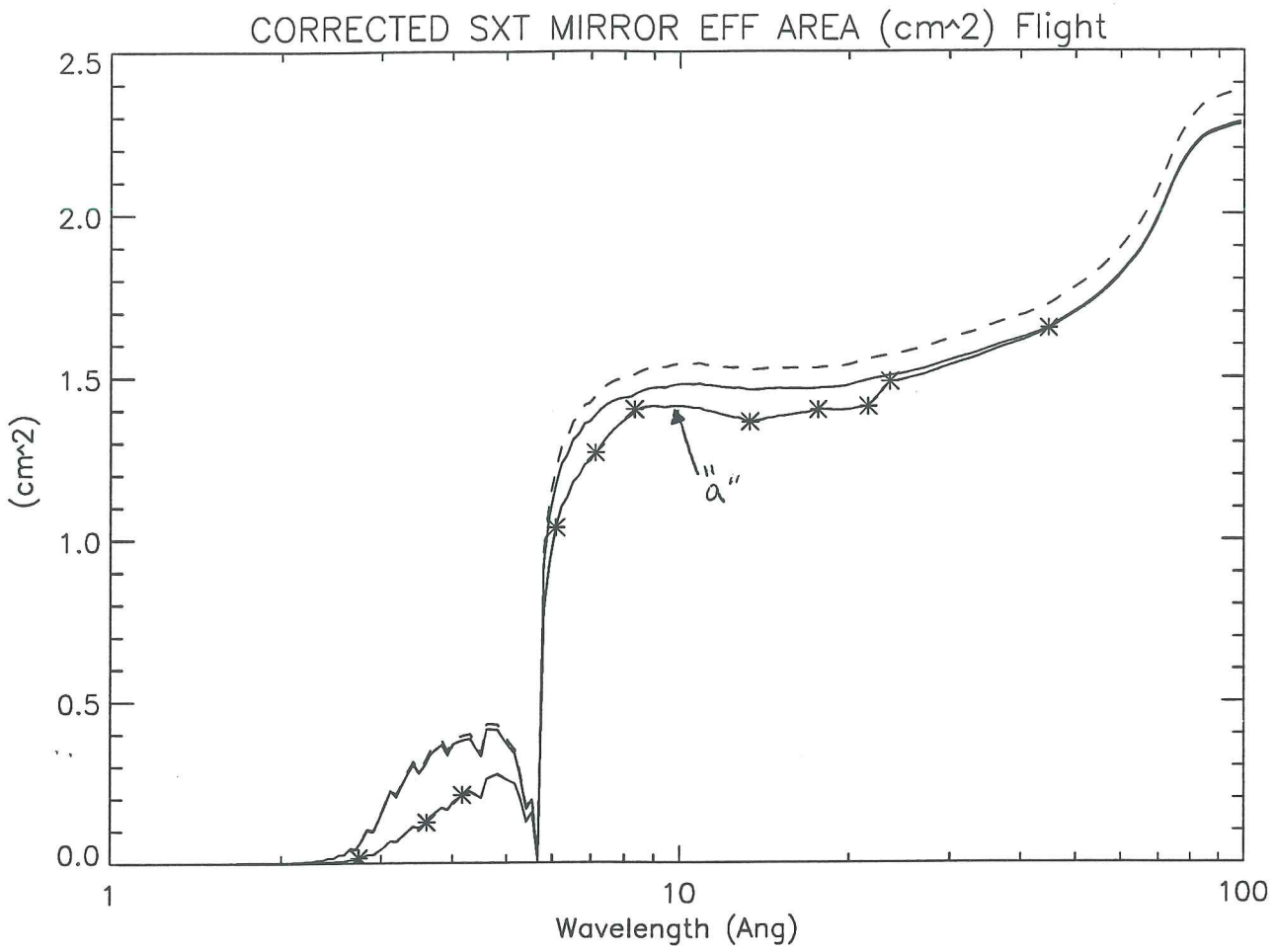

Figure 3: The data points are the effective areas at 11 wavelengths obtained during the June 1989 MSFC2 measurements, except that they have been multiplied by the ratio of the Flight configuration obscuration over the MSFC obscuration (= .93882 / .97883). The curve that runs through the data points is Theory Calculation 2 (infinity focus and flight obscuration) multiplied by the linearly interpolated ratios to the measured / Theory Calculation 1 (which is shown as a dashed curve in Figure 2). The solid curve above that (the one just under the dashed curve) is Theory Calculation 2 (infinity focus and flight configuration obscuration). The dashed curve is the area that was used to compute the SXT sensitivity response in July 1991. This curve is makes use of the infinity focus ray trace model, but uses the MSFC obscuration factor. This calculation is not appropriate and should not be used in future analyses.

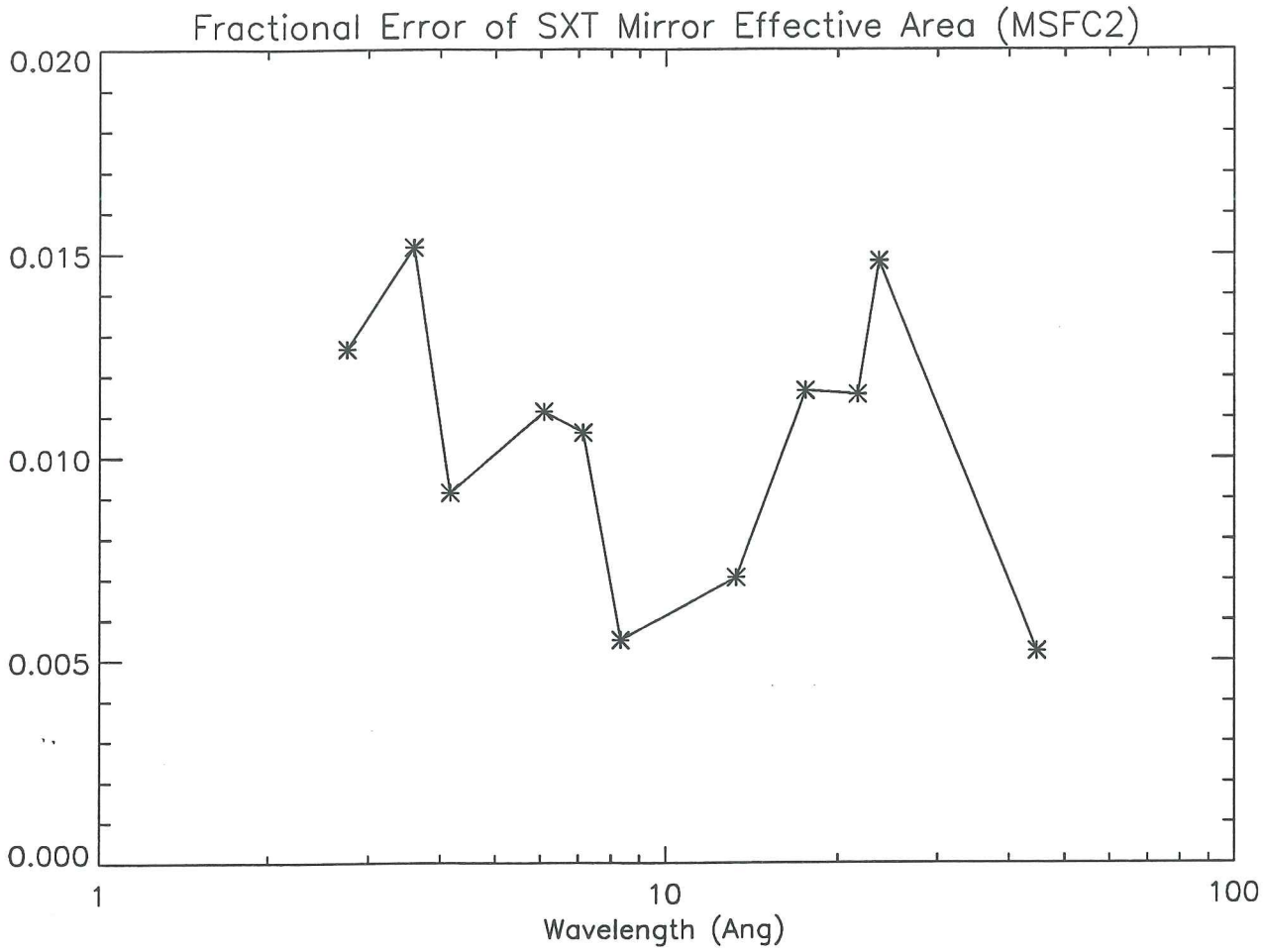

Figure 4: The fractional error of the effective area measurements of the SXT mirror made at MSFC2. The uncertainty is due to the counting statistics. The data is taken from Table 1. The average error is 0.01 for the 11 measurements.